

A model for the resistance of the proton channel formed by the proteolipid of ATPase

Z. Schulten and K. Schulten

Physik-Department, Technische Universität München, D-8064 Garching, Federal Republic of Germany

Received April 6, 1984/Accepted August 31, 1984

Abstract. The conductance observed for single proton channels formed by proteolipids of ATPase (Schindler and Nelson 1982) is rationalized in terms of a hydrogen bonded network model. A simple algebraic expression for the resistance predicted for such a model is presented and the results are compared to the experimental observations. The comparison suggests that the conduction involves a series of bound water molecules and perhaps amino acid side groups.

Key words: Proton channel, hydrogen-bonded network, resistance

1. Introduction

The conductance of single proton channels formed by the proteolipid of ATPase from yeast mitochondria, after reconstitution into planar bilayers, has recently been measured by Schindler and Nelson (1982). For low proteolipid concentrations and in the absence of cholesterol, these authors observed that the conductance normalized by the proton concentration remains approximately constant upon a symmetric pH change on both sides of the membrane. Around a pH value of 4.5 an increase of the normalized conductance has been recorded for various lipids. We will show in this paper now from these observations the pK values of the groups constituting the proton channel, as well as the kinetic constants of the elementary molecular processes involved in the conductance, can be estimated. For this purpose we provide an analytical expression for the resistance of a proton channel in terms of its molecular properties and compare the results to the measured conductance values as obtained by Schindler and Nelson (1982). The theoretical description will be based on a model introduced now.

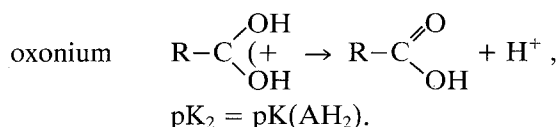
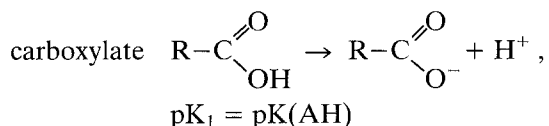
2. Model of the proton channel

Recently, several authors have investigated theoretically the transport properties of proton channels formed by a transmembrane protein (Nagle and Nagle 1983; Brünger et al. 1983). Following a model originally suggested by Onsager (1967), these studies assume that proton channels are constituted by linear hydrogen bonded systems formed from the amino acid side groups of the membrane proteins. In the case of the proteolipid of ATPase the components are the amino acids with polar, uncharged side groups, e.g., threonine, tyrosine, and asparagine; the amino acids with charged, polar side groups, such as aspartic acid; and any molecules of bound water present in the channel as an integral part of the conductor. It is generally accepted that at least two proteolipids are required to form a channel and that the aspartic (glutamic) acid residues are a key component of the proton channel (Sebald et al. 1979; Hoppe and Sebald 1984). The native proton channel, i.e. the F_0 fraction of ATPase, appears to function only when in addition to the proteolipids, two further protein subunits are present. The observations of Schindler and Nelson (1982) indicate that the proteolipid alone, albeit in pairs, form proton channels in artificial membranes although the possibility of non-specific water channels forming spontaneously in the membrane at low pH cannot be disregarded.

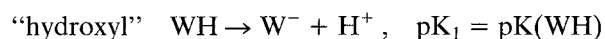
Sequence and structural studies indicate that the aspartic acid residue is located roughly in the middle of the membrane (Hoppe and Sebald 1984; Sebald and Wachter 1979; Senior 1983; Sebald and Hoppe 1981). Since the proteolipid appears to be a hairpin α -helix with largely hydrophobic segments crossing the membrane, the two proteolipids *may be nested* together in order to utilize the largest number of hydrogen bonding side groups for the proton transport. Hoppe and Sebald (1984) have recently suggested that a proton channel could be totally

constructed from water molecules that are bound either by the amino acid side groups or by the polar groups of the peptide bonds. Since the exact arrangement is not known and it is difficult to differentiate kinetically the transport of a proton by a bound water molecule from transport by an organic hydroxyl group such as in threonine, we will consider the following simple model:

The channel consists of N groups with the centre group representing a cluster of one or more aspartic acid side chains. Each group in the channel has two states of protonation and correspondingly two pK values. For aspartic acid the pK values describe the formation of the carboxylate and oxonium ions



The other conductor groups (WH) are assumed to be either *bound water* or *polar side groups* and their two states of protonation are



We will assume below $pK(\text{AH}_2) = pK(\text{WH}_2)$ and will find that in the pH range $1 \leq \text{pH} \leq 5$ that $pK(\text{AH})$ and $pK(\text{WH})$ do not contribute to the conduction. Therefore, in this range the model can also be reconciled with a channel formed solely by molecules of water.

The conductor model is represented schematically in Fig. 1 which shows the corresponding chain of hydrogen bonded groups. At thermal equilibrium at acidic pH one finds one proton in each hydrogen bond, and the two most probable proton configurations are those shown in Fig. 1, in which the protons are situated either all to the right side or all to the left side of the groups. In analogy with the experimental situation (Schindler and Nelson 1982) we will assume in our calculations that the pH values of the solutions on either side of the membrane are titrated symmetrically and that proton transport is induced by a voltage difference applied across the membrane. The transport will primarily involve the series of proton configurations shown in Fig. 2a. The symbols OO, OX, XO, XX represent the four possible protonation states of a single group, i.e., no proton, one proton to the right, one proton to the left, and protons on both

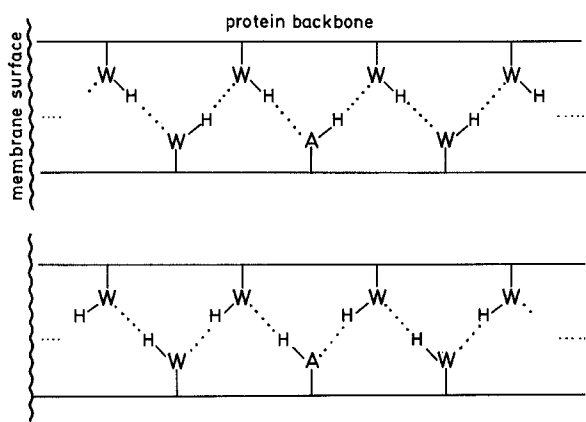


Fig. 1. Model of the proton channel formed by the proteolipids of ATPase. The center group is assumed to be a carboxylate side group of aspartic acid. The neighbouring groups (WH) are either bound water or amino acid side groups. The two equilibrium proton configurations in the hydrogen bonded network in which the protons are situated all to the right (a) and all to the left (b) of the groups are shown

sides of the respective group. The symbol OX OX OX OX OX represents the equilibrium configuration denoted by $c(1)$ with all protons to the right side of the groups, XO XO XO XO XO represents the other equilibrium configuration denoted by $c(N+2)$ with all protons to the left side of the groups. We choose the symbols $c(i)$, $i = 2, 3, \dots$ to represent further proton configurations. Figure 2a presents two pathways of proton configurations along which protons can be conducted. In the top pathway of Fig. 2a an excess proton enters the channel at the left-hand side denoted by the transition $c(1) = \text{OX OX OX OX OX} \rightarrow c(2) = \text{XX OX OX OX OX}$. The excess proton XX is then transported across the membrane by a series of $N-1$ jumps between the groups, e.g., $\text{XX OX OX OX OX} \rightarrow \text{OX XX OX OX OX}$. At the right side the excess proton is released into the solution as described by the transition $c(N+1) = \text{XO XO XO XO XO} \rightarrow c(N+2) = \text{XO XO XO XO XO}$, i.e., the conductor enters an equilibrium configuration. In the bottom pathway of Fig. 2a a proton jumps between the two central groups of the conductor and, thereby, creates a double fault of an excess proton XX and an empty group OO. These states correspond to the carboxylate anion of the aspartic acid and the hydronium-like ion on its neighbouring residue. The excess proton XX wanders to the right-hand side where it will be given off to the solution. An excess proton then enters the conductor from the left-hand side and wanders to the centre where it combines with the carboxylate anion. These events leave the conductor again in the equilibrium configuration $c(N+2)$.

In order to return the conductor for either pathway from $c(N+2)$ back to the equilibrium

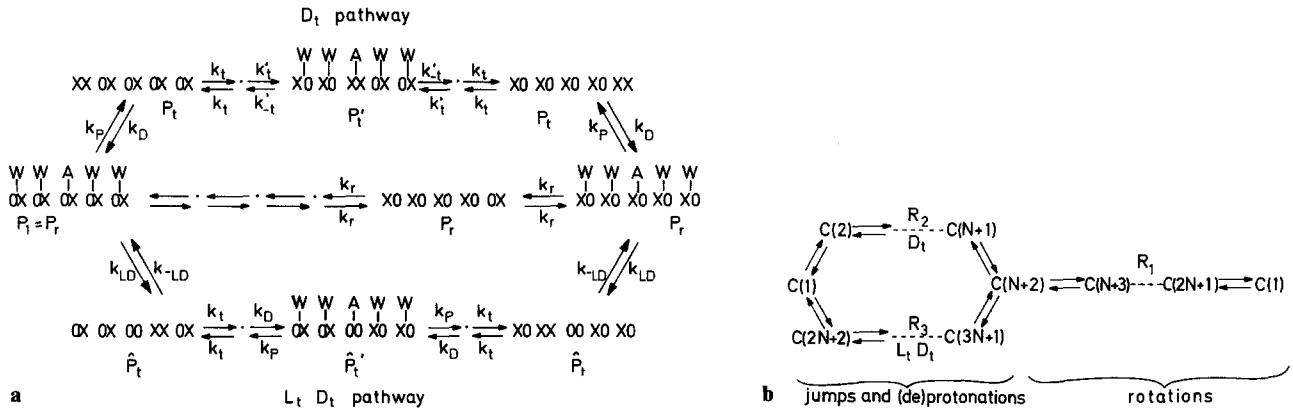


Fig. 2. **a** Kinetic diagram of the proton configurations involved in the transport of protons for a channel formed by five groups. The symbols X (0) represents the case that a proton (no proton) is situated at one of the two possible binding sites of each group. The rate constants which govern the transitions between the proton configurations, e.g., k_r and k_t are shown; here the index r refers to rotation and t to jump processes, P and D denote protonation–deprotonation processes at the end groups and LD the transfer of a proton between the aspartic acid central group and one of its neighbouring groups. Several intermediate configurations denoted by (*) have been omitted. **b** Schematic representation of the two pathways of proton transport in **a** for a channel composed of N groups. $c(i)$ denote the individual proton configurations. The resistance corresponding to this diagram can be evaluated according to Kirchhoff's rules interpreting the pathways as an electrical network. The resistance attributed to the three unbranched parts of the network are indicated (see text)

configuration $c(1)$, successive *rotations* or *reorientations* of the single groups are necessary. This part of the conduction is then common to both pathways. The resulting two conduction mechanisms are represented schematically in Fig. 2b. Since the transport in the top pathway of Fig. 2a, b involves the oxonium- and hydronium-like excess protons XX, so-called double ionic faults D_t , this pathway has been labelled D_t . Since the conduction along the bottom pathway in Figs. 2a, b involves the simultaneous formation of an empty group as well as an excess proton, the bottom pathway has been labelled $L_t D_t$.

3. Resistance of a proton channel

In a previous publication (Brünger et al. 1983) we derived an expression for the resistance of a proton channel near thermal equilibrium, i.e., for small voltage differences, V , across the membrane. This expression holds for a linear voltage-current relationship $V = RI$, where R measures the resistance of the channel and I the proton current. Applied to the kinetic pathways shown in Fig. 2b the resistance is

$$R = R_1 + (1/R_2 + 1/R_3)^{-1}, \quad (2)$$

where

$$R_i = (kT/e) \sum_{j \in M_i} 1/(K_{j \rightarrow j+1} P_j). \quad (3a)$$

R_i is the resistance contributed along each unbranched segment of the kinetic pathways in Fig. 2b, which are combined according to Kirchhoff's rules of networks. The resistance R_1 accounts for the

rotations, i.e., involves the configurations

$$M_1 = (N + 2, N + 3, \dots, 2N + 1, 1), \quad (3b)$$

R_2 for jumps and (de)protonations along the D_t pathway involving the configurations

$$M_2 = (1, 2, \dots, N + 2),$$

and R_3 for jumps and (de)protonations along the $L_t D_t$ pathway involving the configurations

$$M_3 = (1, 2N + 2, \dots, 3N + 1, N + 2).$$

P_j is the probability for the j -th proton configuration to appear in thermal equilibrium. $K_{j \rightarrow j+1}$ are the first-order rate constants describing the transition $c(j) \rightarrow c(j+1)$ at thermal equilibrium, i.e., when no voltage is applied. We assume that the elementary processes of proton jumps between groups, e.g., $OX \rightarrow OO$, $OO \rightarrow OO XO$, and group rotation, e.g., $OX \rightarrow XO$, are thermally activated events which follow Arrhenius's law

$$K_{j \rightarrow j+1} = A_{j \rightarrow j+1} \exp[-E(j \rightarrow j+1)/kT], \quad (4)$$

where $A_{j \rightarrow j+1}$ is the frequency factor and $E(j \rightarrow j+1)$ the energy of activation for the transition. The assignment of values for the rate constants has been discussed (Nagle and Nagle 1983; Brünger et al. 1983), and we provide the values employed in our calculations in Table 1.

The rate constants for the rotation of a single group $k_r \approx 10^{10} \text{ s}^{-1}$ and for the jump of a proton between neighbouring groups $k_t \approx 10^{11} \text{ s}^{-1}$ are in agreement with the values suggested by Nagle and Nagle (1983) in their recent review on theoretical

Table 1. Activation barriers (E_A) and rate constants (k) for the elementary transport processes

Motion jumps	E_A [eV]	k [10^{10} s^{-1}]
k_t (k'_t)	0.02	23
k'_t	$0.02 + 2.3 [\text{pK}(\text{AH}_2) - \text{pK}(\text{WH}_2)]/\beta$	
k_{LD}	$0.04 + 2.3 [\text{pK}(\text{AH}) - \text{pK}(\text{WH}_2)]/\beta$	
k_{-LD}	0.04	11
Rotation k_r	0.10	1.0

models of proton pumps and ATPases. While the jumps are generally accepted to be picosecond motions, the time scale for the reorientation or rotation of a side group can vary over many orders of magnitude depending on its location within the protein. For example, subnanosecond rotations of tryptophan (not a hydrogen bonding group) residues located in the hydrophobic interior of a protein have been reported (Munro et al. 1979). Mackay et al. (1984) observed in a recent molecular dynamics study of the gramicidin A channel that a linear hydrogen bridge chain of water molecules forms in this channel with a rotational relaxation time of a few picoseconds. However, Wagner et al. (1976) have determined by means of NMR spectroscopy that the rings of tyrosine and phenylalanine groups in globular proteins rotate with rate constants in the microsecond range.

The analysis below shows that the observed proton conductance of channels of ATPase proteolipids can be reproduced only if one assumes a rate constant of 10^{10} s^{-1} for rotation. The correspondingly fast rotations for these channels involve the aspartic acid side groups, and either bound water or threonine, and asparagine side groups. Since none of these groups are very bulky and in view of the observations and calculations of Munro et al. (1979) and Mackay et al. (1984) the large magnitude of the rate constant may be justified. However, proton conduction through other protonacious hydroxy matrices may be governed by slower side group rotation as has been assumed, for example, by Brunger et al. (1983).

For conductance in an acidic environment ($\text{pH} < 8$) the protonation of the channel end group will depend primarily on the diffusion controlled reaction with the H_3O^+ ions in solution, while the deprotonation step will depend primarily on the proton transfer rate k_t and the group's pK value. With the assumption that the appearance of water as a reactant at the channel entrance is faster than the transfer of a proton, one obtains the following approximate expressions for the rate constant (Brunger et al. 1983) of protonation

$$k_P = \kappa_d 10^{-\text{pH}} \begin{cases} 1/3 & \text{for } \Delta\text{pK}_2 = 0 \\ 1/2 & \text{for } \Delta\text{pK}_2 > 0 \end{cases} \quad (5a)$$

and for the rate constant of deprotonation

$$k_D = k_t/2 \begin{cases} 1 & \text{for } \Delta\text{pK}_2 = 0 \\ 10^{-\Delta\text{pK}_2} & \text{for } \Delta\text{pK}_2 > 0, \end{cases} \quad (5b)$$

where $\Delta\text{pK}_2 = \text{pK}(\text{WH}_2) - \text{pK}(\text{H}_3\text{O}^+)$ and $\kappa_d = 4 \cdot 10^{10} \text{ l/mol} \cdot \text{s}$, a value suitable for proton transfer reactions controlled by three-dimensional diffusion. However, a comparison with the observed proton conductivity below will reveal that protons are injected into the channel at a rate about fourfold faster than described by (5a). Such acceleration of the proton injection process can occur if the proton injection is a two step process involving a diffusive motion towards the membrane surface, and then lateral diffusion towards the channel entrance, possibly guided by negative charges.

If we formally define the energy of injection E_{inj} by

$$k_P/k_D = 10^{\Delta\text{pK}_2 - \text{pH}} \kappa_d/k_t = \exp(-E_{\text{inj}}/kT)$$

one sees immediately that the efficiency of the first step in the transport depends (1) on the external pH, (2) on the pK difference between the end group and the H_3O^+ molecule in solution, and (3) on the ratio t_1/t_2 of the time t_1 for the transfer of the proton ($1/k_t$) from the solution to the end group and the time t_2 which the proton needs to find the entrance of the channel ($\kappa_d 10^{-\text{pH}}$). At $\text{pH} = 5$ one obtains the value $E_{\text{inj}} = 0.33 \text{ eV}$ for $\Delta\text{pK}_2 = 0$.

4. Comparison with experiment

Figure 3 provides a comparison between the proton conductance, $1/R$, as measured by Schindler and Nelson (1982) and as predicted by means of (2). R_0 scales the resistance R and was set to the value $1/20 \text{ pS}$

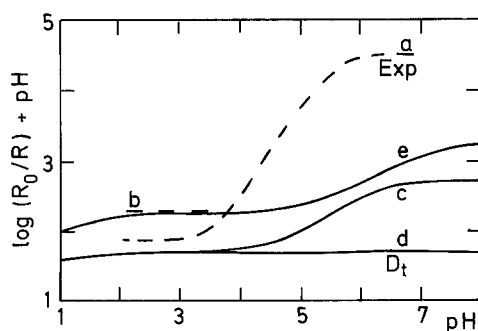


Fig. 3. pH dependence of the conductance $A = 1/R$ predicted for a single proton channel and as observed by Schindler and Nelson (1982). The scale factor for the resistance is $R_0 = 1/20 \text{ pS}$, the applied voltage difference is $V = 50 \text{ mV}$. (a) total conductance observed, (b) single channel conductance extrapolated from (a) (see text), (c–e) theoretical predictions for a channel with $n = 11$ groups, (d) contribution of the D_t cycle alone (see Fig. 2), (e) like (c) but with κ_d increased fourfold

used by Schindler and Nelson (1982). The conductance has been normalized by a factor 10^{pH} in order to eliminate that trivial part of the pH dependence of the conductance which increases linearly with the proton concentration. This dependence originates from the protonation steps in the conduction pathways in Fig. 2. As long as the protonation steps are rate determining for the overall proton transport the conductance will be proportional to the proton concentration, i.e., the normalized conductance should be constant.

For a comparison between observed and calculated conductances one has to abstract from the observation that conductance which refers to single channels. The data of Schindler and Nelson (1982) refer in part to the total conductance and can involve situations where channels are only partly open or where more than one channel is open. The increase by about two orders of magnitude of the observed total conductance in Fig. 3 is seen only with membranes prepared with cholesterol and with a high proteolipid concentration. Schindler and Nelson (1982) state that this increase is probably due to an increase in the number of channels in the pH range above 4 rather than due to an increase of the single channel conductance. Accordingly the data imply only a weak pH dependence of the conductance below $\text{pH} = 4$ and are inconclusive about the pH-dependence under neutral and basic conditions. The authors also state that their membrane at low pH values contain on average, 0.44 open single channels. The absolute single channel conductance should then be larger by a factor 2.3. The resulting conductance value is indicated in Fig. 3.

Figure 3 presents two theoretical conductance curves, both based on $n = 11$ conductor groups. The lower conductance values (c–d) result from the kinetic constants of Table 1 and (5). The higher conductance values (e) which agree closely with the extrapolated single channel conductance (b) of Schindler and Nelson (1982) assumes a rate constant k_p of proton injection which is larger by a factor 4. This increase of k_p , which leaves the pH-dependence of the conductance nearly unaltered, is invoked solely to fit the experimental data but can be rationalized as discussed in Sect. 3. We have indicated for the lower conductance values in Fig. 3 the separate contributions to the channel conductance of the D_i and of the $L_i D_i$ pathways in Fig. 2. If the protons are transported solely by the D_i mechanism the calculated conductance remains constant for $\text{pH} > 1$. Using the notation provided in Fig. 2a the resistance obtained from (2) and (3) of the kinetic cycle involving the D_i mechanism is, for N conductor groups

$$R = \Omega [N/k_r P_r + (N-3)/k_i P_i + 2/k_i' P_i + 2/k_D P_i] \quad (6)$$

where $\Omega = kT/e$ and $k_i' = k_i 10^{-\text{pK}(\text{WH}_2) + \text{pK}(\text{AH}_2)}$. In deriving (6) we have employed the detailed balance conditions $k_p P_r = k_D P_i$ and $k_{-i}' P_i' = k_i' P_i$. For $\text{pH} \gg \text{pK}(\text{WH}_2)$ or, equivalently, for $k_D/k_p \gg 1$ the resistance of the rotational sequence $R_1 = N/k_r P_r$ is negligible in comparison to the contribution from the remaining transitions, and the total resistance is approximately

$$R \simeq R_2 = \Omega 10^{\Delta \text{pK}_2 + \text{pH}} (k_i/\kappa_d)(N+1)[(N-3)/k_i + 2/k_i' + 2/k_D] \quad (7)$$

To obtain this expression we employed (5) and the detailed balance conditions given above. In the limit considered $k_D \gg k_p$ the proton configurations in the rotational sequence, e.g., XO XO XO XO OX, are the most probable and $P_r = 1/(N+1)$, which follows from the normalization condition $(N+1)P_r + NP_i = 1$ and $P_i \sim 0$.

If we assume that the dissociation constant of the aspartic oxonium ion (AH_2^+) and the hydronium-like ions (WH_2^+) are similar then the difference between the effective pK values of these groups will provide only a small contribution to the resistance. The respective dissociation constants for unsubstituted amides are typically -1 , and, for convenience, we assume the value -1.74 for all groups so that $\Delta \text{pK}_2 = 0$ in the calculations presented in Fig. 3. If the groups (W) should be more basic, e.g., $\text{pK}(\text{WH}_2) = 0$, the deprotonation term would dominate the resistance. In this case the conductance would be slightly larger than shown in Fig. 3. The groups cannot be too basic, however, since the D_i pathway yields a pH independent normalized conductance in the range $2 < \text{pH} < 7$ only for $\text{pK}(\text{AH}_2) \leq \text{pK}(\text{WH}_2) < 0$, i.e., groups which are more basic yield a pH-dependent conductance in a pH range where there is none observed.

Since the rate constants for deprotonation, k_D , and proton transfer to the aspartic acid residue are on the order of k_i , the normalized conductance is determined primarily by the fast rate of hopping, k_i , and the diffusion-controlled rate constant, κ_d . Since in Fig. 3 the pK_2 values of all groups were chosen to be identical, the dependence on the hopping rate in (7) cancels out and the resistance will depend solely on the diffusion-controlled rate constant, on N and on the pH. The contribution of the length to the normalized conductance is $-\log(N+1)$ and this length dependence is not very important since N should be less than 30. The conductance of the D_i pathway in Fig. 3 is then typical of a non-specific water channel since the values $\text{pK}(\text{AH})$ and $\text{pK}(\text{WH})$ do not contribute to the conductance.

In the case where both mechanisms in Fig. 2 contribute significantly to the proton transport the

calculated normalized conductance will exhibit a slight increase at a pH near the dissociation constant of the aspartic acid, i.e., at $\text{pH} = 4.5$ for the conditions assumed in our calculations. The resistance of the rotational sequence can be neglected over the entire pH range. For $1 < \text{pH} < \text{pK}(\text{AH})$ the resistance of the protonation–deprotonation processes and proton jumps between groups in the $L_i D_i$ pathway is so large that the conductance is solely determined by the resistance R_2 , of the D_i pathway. For $\text{pH} > \text{pK}(\text{AH})$ the resistance of the $L_i D_i$ pathway R_3 is smaller than that of the D_i pathway and the proton transport is determined primarily by the $L_i D_i$ mechanism. In this pH range the major contribution to the resistance comes from the sequence of (de)protonation processes and proton jumps, and the following equation for the resistance holds

$$R \approx R_3 = \Omega 10^{4\text{pK}_2 + \text{pH}} (k_t/\kappa_d) [2/k_{-LD} + (N-3)/k_t + 2/k_D]/\hat{P}_i' \quad (8)$$

In this expressions \hat{P}_i' is the probability that the channel exists in a state such that the aspartic acid side group is dissociated and the hydrogen bridge network to its left and right is intact (see Fig. 2). The probabilities in Fig. 2 obey the normalization condition $(N+1)P_r + \hat{P}_i' + (N-1)\hat{P}_t + NP_i = 1$. For $\text{pH} > \text{pK}(\text{AH}) - \text{pK}(\text{H}_3\text{O}^+)$, \hat{P}_i' is approximately one. The pH range of the conductance increase shifts to higher pH values as the dissociation constant of the aspartic acid side group is increased. The height of the second conductance plateau above the first plateau depends only on the number of groups N and on the rate constant k_{-LD} for the reprotonation of the carboxylate ion from the neighbouring group. For the rate constants given in Table 1, $k_{-LD} \approx k_t$ and R_3 is approximately $(N+1)$ times smaller than R_2 .

The question arises as to whether or not the mechanism which induces a pH-dependence of the theoretical proton conductance at $\text{pH} = 4.5$ could also contribute to the aggregation of proteolipids observed in this pH range by Schindler and Nelson (1982). For a positive answer one may consider that aggregation is facilitated by the charged proton configuration \hat{P}_i' which at $\text{pH} > 4$ is stabilized relative to the other proton configurations and, thereby, may contribute to the aggregation of the proteolipids and open the second ($L_i D_i$) conduction pathway.

5. Discussion

We have calculated the resistance as a function of pH for a model of the single proton channel formed by the proteolipid of ATPase. The model assumes that protons are transported through a linear hydrogen

bonded network formed from bound water and the amino acid side groups of the protein. The calculations are based on simple algebraic expressions [(2)–(7)] which relate the resistance to the kinetic properties of elementary processes within the channel, e.g., proton jumps between neighbouring groups, and rotation of groups, as well as to the pK values of the groups. These expressions hold within the range of a linear voltage–current relationship. The processes are difficult to observe directly. The single channel measurements of Schindler and Nelson (1982) allow the first direct comparison with the predictions of the above channel model and, thereby, should provide information on the functional constituents and elementary dynamic processes of proton channels. The comparison reveals that the magnitude of the single channel proton conductance can be accounted for by the model and is determined mainly by the jumps of protons between neighbouring groups and the protonation–deprotonation processes at the endgroups.

The comparison of the experimental curve with the theoretical expressions for the conductance reveals that the rotation of the groups, necessary for the conductance process, should be rather fast. Otherwise, if the rate constants for group rotation were considerably smaller than 10^{10} s^{-1} the observed pH dependence of the conductance would not be reproduced. This finding implies that the hydrogen bonds between the conductor groups are weak. The necessity for fast rotations is consistent with a model of the proton channel constructed from bound water and flexible amino acid side groups such as threonine and asparagine and would imply that the amino acid side groups with aromatic rings are not involved in the transport. At the low pH range considered by Schindler and Nelson (1982), the conduction can be reconciled with a channel formed solely by molecules of water and, hence, might be non-specific. The comparison with the data of Schindler and Nelson (1982) further reveals that the rate of proton injection should be fast, such that one needs to invoke local surface diffusion for an explanation of the corresponding rate constant.

The deviations from Ohm's law that Schindler and Nelson (1982) report can be attributed in part to the voltage dependence of the rate constant for proton jumps between groups. Since the activation barrier for proton jumps is likely to be small (see Table 1) applying an external voltage which induces a lowering of the activation energy could easily lead to a saturation of the rate constant because 'negative' activation energies should not increase a rate constant.

When both (D_i and $L_i D_i$) conduction mechanisms indicated in Fig. 2 contribute to the proton transport,

which should be the case for “in situ” pK_1 values of aspartic acid below 7, a slight increase of the conductance is predicted to occur at a pH value around this pK_1 . The increase depends on the number of groups N forming the channel as well as on the pK difference between the central aspartic acid side group and the remaining conduction groups. Since the difference is proportional to $\log N$, a large increase in the conductance with pH cannot occur. To explain the large increase in the conductance $\Lambda(\text{pH})$ at higher pH, we would have to assume, as do Schindler and Nelson (1982), that they are measuring the total conductance $\Lambda(\text{pH}) = M(\text{pH})\lambda_s$ where $\lambda_s = 1/R$ is the conductance of the single channel and $M(\text{pH})$ is the number of open channels. $M(\text{pH})$ is dependent on pH and can increase due to aggregation of the proteolipids.

References

- Brünger A, Schulten Z, Schulten K (1983) A network thermodynamic investigation of stationary and non-stationary proton transport in proteins. *Z Phys Chem NF* 136: 1–63
- Hoppe J, Sebald W (1984) The proton conducting F_0 part of bacterial ATP synthesis. *Biochim Biophys Acta* 768: 1–27
- Mackay D, Berens P, Wilson K, Hagler A (1984) Structure and dynamics of ion transport through gramicidin A. *Biophys J* 46: 229–248
- Munro I, Pecht I, Stryer L (1979) Subnanosecond motions of tryptophan residues in proteins. *Proc Natl Acad Sci USA* 76: 56–60
- Nagle J, Nagle S (1983) Hydrogen bonded chain mechanisms for proton conduction and proton pumping. *J Membr Biol* 74: 1–14
- Onsager L (1967) Thermodynamics and some molecular aspects of biology. In: Schmitt FO (ed) *The neurosciences*. Rockefeller University Press, New York, pp 75–79
- Schindler H, Nelson N (1982) Proteolipid of adenosinetriphosphatase from yeast mitochondria forms proton-selective channels in planar lipid bilayers. *Biochemistry* 21: 5787–5794
- Sebald W, Graf T, Lukins HB (1979) The DCCD-binding protein of the mitochondrial ATPase complex from neuro-spora crassa. *Eur J Biochem* 93: 587–599
- Sebald W, Hoppe J (1981) On the structure and genetics of the proteolipid subunit ATP synthase complex. *Curr Top Bioenerg* 12: 1–64
- Sebald W, Wachter E (1979) Amino acid sequence of the putative protonophore of the energy-transducing ATPase complex. In: Schafer G, Klingenberg M (eds) *Energy conservation in biological membranes*. Springer, Berlin Heidelberg New York, (Colloquium Mosbach Ser. vol 29) pp 228–236
- Senior A (1983) Secondary and tertiary structure of membrane proteins involved in proton translocation. *Biochim Biophys Acta* 726: 81–95
- Wagner G, Demarco A, Wüthrich K (1976) Dynamics of aromatic amino acid residues in the globular conformation of the basic pancreatic trypsin inhibitor. *Biophys Struct Mech* 2: 139–158